Spontaneous abrupt climate change due to an atmospheric blocking–sea-ice–ocean feedback in an unforced climate model simulation

Sybren Drijfhout[a,b,1], Emily Gleeson[c], Henk A. Dijkstra[d], and Valerie Livina[e]

[a]Department of Climate Research, Royal Netherlands Meteorological Institute, 3730AE, De Bilt, The Netherlands; [b]School of Ocean and Earth Sciences, National Oceanography Centre, Southampton SO14 3TB, United Kingdom; [c]Research, Environment and Applications Division, Met Éireann, Dublin 9, Ireland; [d]Institute for Marine and Atmospheric Research Utrecht, Utrecht University, 3584 CC Utrecht, The Netherlands; and [e]National Physical Laboratory, Teddington TW11 0LW, United Kingdom

Edited by Mark H. Thiemens, University of California at San Diego, La Jolla, CA, and approved October 18, 2013 (received for review March 15, 2013)

Abrupt climate change is abundant in geological records, but climate models rarely have been able to simulate such events in response to realistic forcing. Here we report on a spontaneous abrupt cooling event, lasting for more than a century, with a temperature anomaly similar to that of the Little Ice Age. The event was simulated in the preindustrial control run of a high-resolution climate model, without imposing external perturbations. Initial cooling started with a period of enhanced atmospheric blocking over the eastern subpolar gyre. In response, a southward progression of the sea-ice margin occurred, and the sea-level pressure anomaly was locked to the sea-ice margin through thermal forcing. The cold-core high steered more cold air to the area, reinforcing the sea-ice concentration anomaly east of Greenland. The sea-ice surplus was carried southward by ocean currents around the tip of Greenland. South of 70°N, sea ice already started melting and the associated freshwater anomaly was carried to the Labrador Sea, shutting off deep convection. There, surface waters were exposed longer to atmospheric cooling and sea surface temperature dropped, causing an even larger thermally forced high above the Labrador Sea. In consequence, east of Greenland, anomalous winds changed from north to south, terminating the event with similar abruptness to its onset. Our results imply that only climate models that possess sufficient resolution to correctly represent atmospheric blocking, in combination with a sensitive sea-ice model, are able to simulate this kind of abrupt climate change.

climate modeling | thermohaline circulation | Great Salinity Anomaly

A common definition of abrupt climate change is that the climate is undergoing a transition at a faster rate than changes in the external forcing. Dansgaard–Oeschger (DO) events are the iconic examples of such abrupt climate change, featuring the last glacial period as recorded in Greenland ice cores (1). DO events have been linked to large variations of the Atlantic meridional overturning circulation (AMOC), forced by freshwater input into the North Atlantic (2). This theory has been corroborated by results from coarse-resolution climate models with simplified atmospheric dynamics (3, 4). However, more sophisticated climate models show a temperature response that is still weak compared with DO events (5), even in the case of unrealistically large freshwater forcing. Recently, it has been argued that sea ice might play a key role in the onset of DO events (6, 7). A displacement of the ice edge rapidly changes the amount of absorbed shortwave radiation due to the ice–albedo feedback, but also it reduces heat release from the ocean to the atmosphere. Both processes cool the atmosphere and the ocean surface. Series of interactions between ocean and cryosphere may build and erode a freshwater halocline in the Nordic seas, promoting large changes in sea ice that can be associated with changes between cold stadials and warm interstadials (8). In this scenario, the AMOC continues to transport heat northward, but the warm, salty layer is inaccessible to the atmosphere when the surface halocline is present. As a result, subsurface warming takes place below the surface halocline, which eventually destabilizes the water column and erodes the surface halocline.

The link between multiple sea-ice states and AMOC was also investigated within an idealized coupled climate model (9). The sea-ice switch featured abrupt transitions between a weak and strong AMOC, essentially showing that these two mechanisms cannot be considered in isolation. In realistic climate models, the response to a collapse of the AMOC is determined by a fast atmospheric feedback, consisting of reduced greenhouse forcing by a drier and colder atmosphere, mediated through increased sea-ice cover that causes a reduction in evaporation (10). The change in sea ice, in turn, invokes a southward displacement of the Intertropical Convergence Zone, associated with a changed Hadley circulation (11), a scenario that underscores the relation between sea-ice, AMOC, and atmospheric feedbacks. Indeed, although the temperature response in classical hosing experiments is often weaker than the observed changes in DO events (12, 13), in some of the more recent freshwater hosing experiments the response was larger (14), possibly determined by the sensitivity of the sea ice in those models (15). However, the chain of feedbacks between AMOC and sea ice is still unclear, in particular the mediating role of atmospheric feedbacks. In many studies that addressed this relationship, atmospheric feedbacks were either absent, or crudely represented. It was implied that a larger response or sensitivity might be acquired with more complete atmospheric dynamics (16). A climate model with sufficient atmospheric feedbacks and a sensitive sea-ice component

EARTH, ATMOSPHERIC, AND PLANETARY SCIENCES

Significance

There is a long-standing debate about whether climate models are able to simulate large, abrupt events that characterized past climates. Here, we document a large, spontaneously occurring cold event in a preindustrial control run of a new climate model. The event is comparable to the Little Ice Age both in amplitude and duration; it is abrupt in its onset and termination, and it is characterized by a long period in which the atmospheric circulation over the North Atlantic is locked into a state with enhanced blocking. To simulate this type of abrupt climate change, climate models should possess sufficient resolution to correctly represent atmospheric blocking and a sufficiently sensitive sea-ice model.

Author contributions: S.D. and E.G. performed research; S.D., E.G., H.A.D., and V.L. analyzed data; and S.D., E.G., H.A.D., and V.L. wrote the paper.

The authors declare no conflict of interest.

This article is a PNAS Direct Submission.

[1]To whom correspondence should be addressed. E-mail: S.S.Drijfhout@soton.ac.uk.

This article contains supporting information online at www.pnas.org/lookup/suppl/doi:10.1073/pnas.1304912110/-/DCSupplemental.

might feature a much stronger coupled atmosphere–sea-ice–AMOC feedback.

Until now, two examples of spontaneous abrupt climate change have been reported. They occurred in models that were much less refined than present-day climate models (17, 18). In those two cases, a strong coupling between the atmosphere, sea ice, and AMOC was absent, and duration and amplitude of the climate transition was much weaker than events reported for the Holocene (19). Here, we report on a much larger abrupt climate transition. The event is comparable to the Little Ice Age (LIA) in amplitude, it is abrupt in its onset and termination, and is characterized by a century during which the atmospheric circulation over the North Atlantic is locked into a state with enhanced blocking. It occurred in a new generation, state-of-the-art climate model (20) and involved a strong feedback between atmospheric blocking, sea ice, and the AMOC.

Spontaneous Abrupt Change

We investigated the output from a 1,125-y preindustrial (PI) control run from the EC-Earth model. In the PI run the AMOC featured a large drift over the first 100 y, with a strong overshoot followed by a quick resumption. After 450 y, an abrupt cooling event occurred, with a clear signal in the Atlantic multidecadal oscillation (AMO). In the instrumental record, the amplitude of the AMO since the 1850s is about 0.4 °C, its SD 0.2 °C (21). During the event simulated here, the AMO index dropped by 0.8 °C for about a century (Fig. 1*A*). The associated surface air temperature (SAT) anomaly in this period was between 1 and 2 °C over the UK and Scandinavia, with the 1 °C contour stretching from Brittany to Saint Petersburg (Fig. 1*B*). Over Greenland, the SAT anomaly typically was 2 °C, strongly increasing toward the south where it reached 4 °C, even 7 °C over the Labrador Sea, colder than the associated sea surface temperature (SST) anomaly (Fig. S1*A*), which was due to increased sea ice. This temperature anomaly was of similar amplitude to the LIA anomaly (22), but its duration was shorter (100 y) than the events associated with the LIA (23).

After the overshoot and adjustment in the first 200 y, the AMOC converged to 16.2 Sverdrup (Sv; 1 Sv = 10^6 m^3 s^{-1}). Between years 450 and 550, the AMOC was 13.7 Sv, not spectacularly lower than its average value (Fig. 2*A*). The change in AMOC, however, exceeded 2.8σ (5σ after applying a 10-y low-pass filter). Deeper down and farther north, the overturning anomaly was larger than the change in maximum overturning. The deep overturning dropped from 9.7 to 5.7 Sv (exceeding 4σ, and 5σ after applying a 10-y low-pass filter). The AMOC shoaled (Fig. 2*B*) and was more affected north of 35°N than farther south. The cold event happened only a few hundred years after the initial conditions and the strong adjustment is shown in Figs. 1*A* and 2*A*. Crucial to the event, however, was sea ice. Sea-ice concentration (SIC) did not show a trend or adjustment phase (Fig. S2*A*), so the event was not a delayed response to the initial adjustment, which was only apparent in the AMOC and North Atlantic SSTs. Those were, however, not instrumental in creating the cold event, they only modified the response once the event began.

The decrease in the AMOC led to reduced temperatures in the Labrador Sea (Fig. S1*A*), an indication of less convective mixing and reduced upward heat transport in this region, as a tight relationship exists between winter mixed-layer depths and the AMOC (24); and as a consequence of reduced convection, there was longer exposure of surface waters to atmospheric cooling. The SST anomaly bears strong similarities to the cold spot in the observed and modeled pattern of global mean temperature rise, attributed to the decline of the AMOC (25). To shut down deep convection, the density of the surface water must decrease. In the temperature range of 7–12 °C, typical for the Labrador Sea, the SST anomaly in degrees Celsius has to be roughly 5 times the sea surface salinity (SSS) anomaly in practical salinity units for density compensation to occur. The SST anomaly was only about twice that of the SSS anomaly (Fig. S1*B*); the density anomaly was therefore mostly determined by the salinity anomaly. The low salinities formed a halocline that prevented deep convection in the Labrador basin. The source of these low salinities was a surplus of melting sea ice, transported from the east of northern Greenland by ocean currents. The sea-ice surplus originated after the sudden onset of a coupled feedback between sea level pressure (SLP) and sea-ice anomalies.

Mechanism of Abrupt Change

Sixty years before the cold event started, 20-y-averaged SLP anomalies featured an anticyclone above the eastern subpolar gyre (Fig. 3*A*). Such an anticyclone is associated with enhanced outgoing longwave radiation (less clouds) and a negative SAT anomaly developed. As a result, the sea-ice margin in the Greenland Sea started shifting southward and the SIC near the

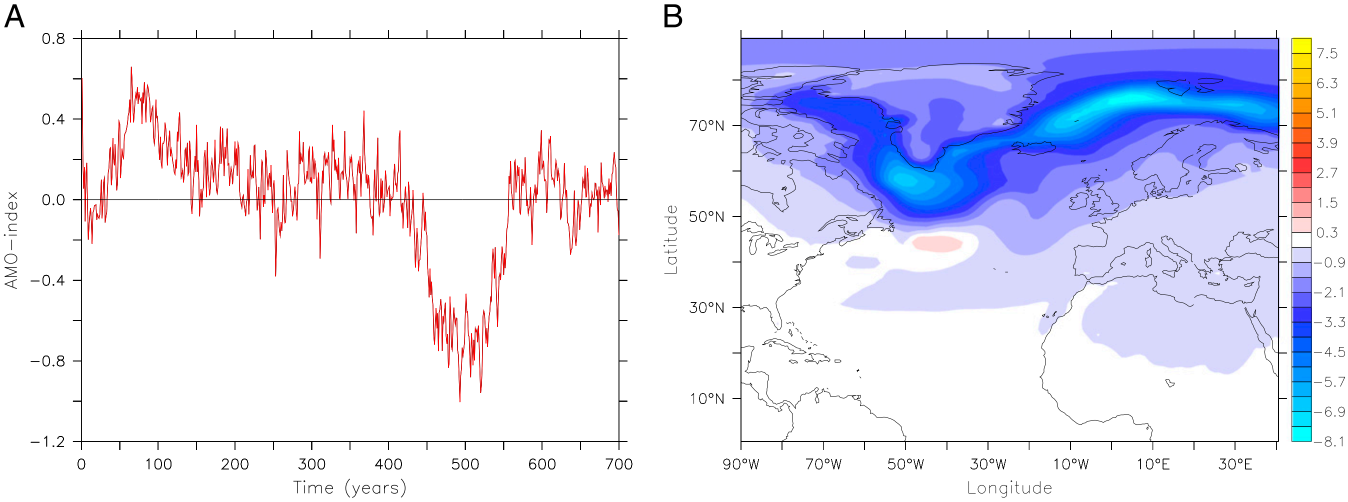

Fig. 1. The temperature signal associated with the cold event. (*A*) Time series of the AMO index, taken as the SST anomaly in the North Atlantic averaged over 0°–70°N in degrees Celsius, relative to the climatology of years 200–400, excluding the first 200-y adjustment phase to the initial conditions. (*B*) Century-averaged SAT anomaly in degrees Celsius over the North Atlantic for years 450–550 (the peak of the cold event) relative to the climatology of years 200–400.

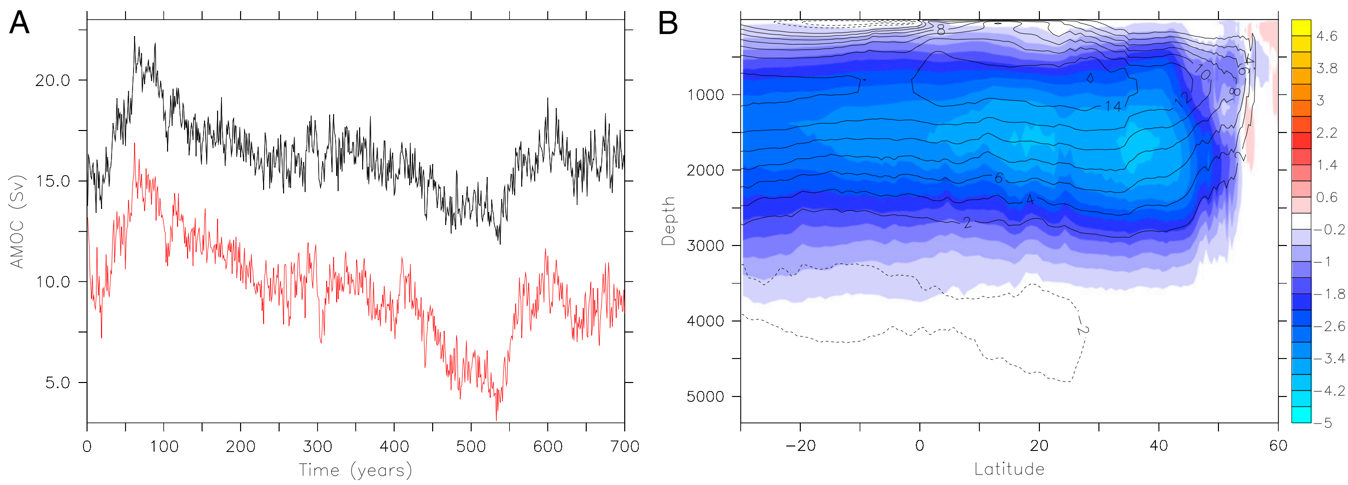

Fig. 2. The AMOC during the first 700 y of the preindustrial run. (*A*) Time series of the AMOC in sverdrups (Sv = 10^6 m^3 s^{-1}). The maximum overturning is in black, and the overturning strength farther north (36°N) and deeper down (1,600 m) is in red and featured the maximum response during the cold event. (*B*) Century-averaged AMOC anomaly for the years 450–550 relative to the climatology of years 200–400 in color scale. The AMOC climatology of years 200–400 is contoured. Both features are displayed as a function of latitude between 30°S and 60°N, and of depth.

sea-ice margin increased. In the following 20 y, the center of the high-pressure anomaly moved in a northeasterly direction toward the sea-ice margin (Fig. 3*B*). Twenty years later, and 20 y before the cold event began, the SIC anomaly displayed a curved band of anomalously high values, stretching from Iceland via Svalbard to Novaya Zemlya (Fig. 4*A*). The northern side of this curved band was associated with a positive ice-production anomaly (less melt), the southern side was associated with increased melt (Fig. S2*C*), indicating that sea ice was carried farther southward by ocean currents before it melted. The SIC anomaly became large enough to be able to excite a high-pressure anomaly, after which the maximum SLP anomaly almost coincided with the SIC anomaly, displaced slightly westward in accordance with theory (Fig. 3*C*). This marked the onset of strong coupling between the SLP and SIC anomalies. The SLP anomaly consisted of a thermally forced cold-core high. Once sea-ice cover extended, the air above cooled, became denser, and sank. Such subsidence is associated with higher pressure. With prevailing westerlies, the SLP anomaly forms east of the forcing area (26). During the height of the cold period the high-pressure system (Fig. 3*D*) steered northerly winds (blowing over a large fetch of sea ice), advecting colder air to the southern sea-ice margin, further increasing SIC. This positive feedback enhanced both the SIC and SLP anomalies. As a result, a similarly larger SIC anomaly developed southwest of Greenland (Fig. 4*B*). The regions of maximum anomalous ice production and melt did not change significantly (Fig. S2*D*), but west of Greenland a zone with a weaker positive ice-production anomaly extended southward into the Labrador Sea, where in the preceding centuries sea ice melted. While SIC anomalies peaked near the sea-ice margin (Fig. 4 *A* and *B*), sea-ice thickness anomalies formed farther north, indicating that the southward progression of the sea-ice margin was due to both increased advection of sea ice from farther northeast of Greenland and slower ice melt during southward advection. The increase of sea ice farther upstream in the Arctic occurred after the SLP anomaly along the ice margin was established. Time series of anomalous ice production and melt in the red- and blue-banded areas in Fig. S2*D* where the anomalies peak, combined with a time series of anomalous sea-ice production in the rest of the Arctic, show no indication of enhanced sea-ice production in the Arctic before sea-ice production anomalies developed east of Greenland (Fig. S2*B*).

These SLP anomalies possess strong high-frequency variability with time series resembling white noise (Fig. S3*B*), and the anticyclones we observe in decadal-to-century averages must be associated with enhanced blocking during these periods and not with continuous high-pressure anomalies. The pressure index that characterizes blocking during the cold event is on average positive and associated with southwesterly winds over the northeast Atlantic storm track. The cold event, however, was characterized by an anomalous negative index (Fig. S3*A*) affecting the southerly component of the winds. The variability of this pressure index is illustrated by its probability density function (Fig. 5*A*), of which the maximum shifted to more negative values and that became narrower and more sharply peaked, especially during the first half of the cold event (years 450–500). The frequency of monthly mean reversals in meridional flow increased in this period, shown by the histogram of blocking frequencies associated with negative pressure indices exceeding 1σ, 1.5σ, and 2σ from the climatological mean (Fig. S3*C*). Shorter-lived and weaker blockings affected the mean values of the monthly mean pressure index by increasing the occurrence of weakly positive values over more strongly positive values (Fig. 5 *A* and *B*). A slightly different index, i.e., the anticyclone south of Svalbard, better represents the trigger of the cold event (Fig. 3*C*). A histogram based on this index shows that the frequency of exceeding the 1σ threshold in the years 425–450 was indeed larger than in any other 25-y period outside the cold event (Fig. S3*D*). In a similar way, an index based on the anticyclone developing above the Labrador Sea (Fig. 3*D*) could characterize the second half of the cold event.

The positive feedback between sea ice and blocking caused anomalies to grow east of Greenland, but growth was limited by advection of sea ice to the southwest. Increasing amounts of sea ice and freshwater from melting sea ice were advected toward the Labrador Sea and subpolar gyre. Because the West Greenland Current is broad and does not extend far north in the model, the Labrador Sea and northwest subpolar gyre are not well separated. Only 23% of the salinity anomaly in the Labrador Sea/subpolar gyre was accounted for by locally melting sea ice. The remainder was due to advection of freshwater that resulted from ice melt between 72°N and the southern tip of Greenland. In the Labrador Sea, a feedback from reduced convection and upward mixing of heat occurred, causing the SST anomaly to amplify, and causing the sea-ice cover anomaly to grow due to

EARTH, ATMOSPHERIC, AND PLANETARY SCIENCES

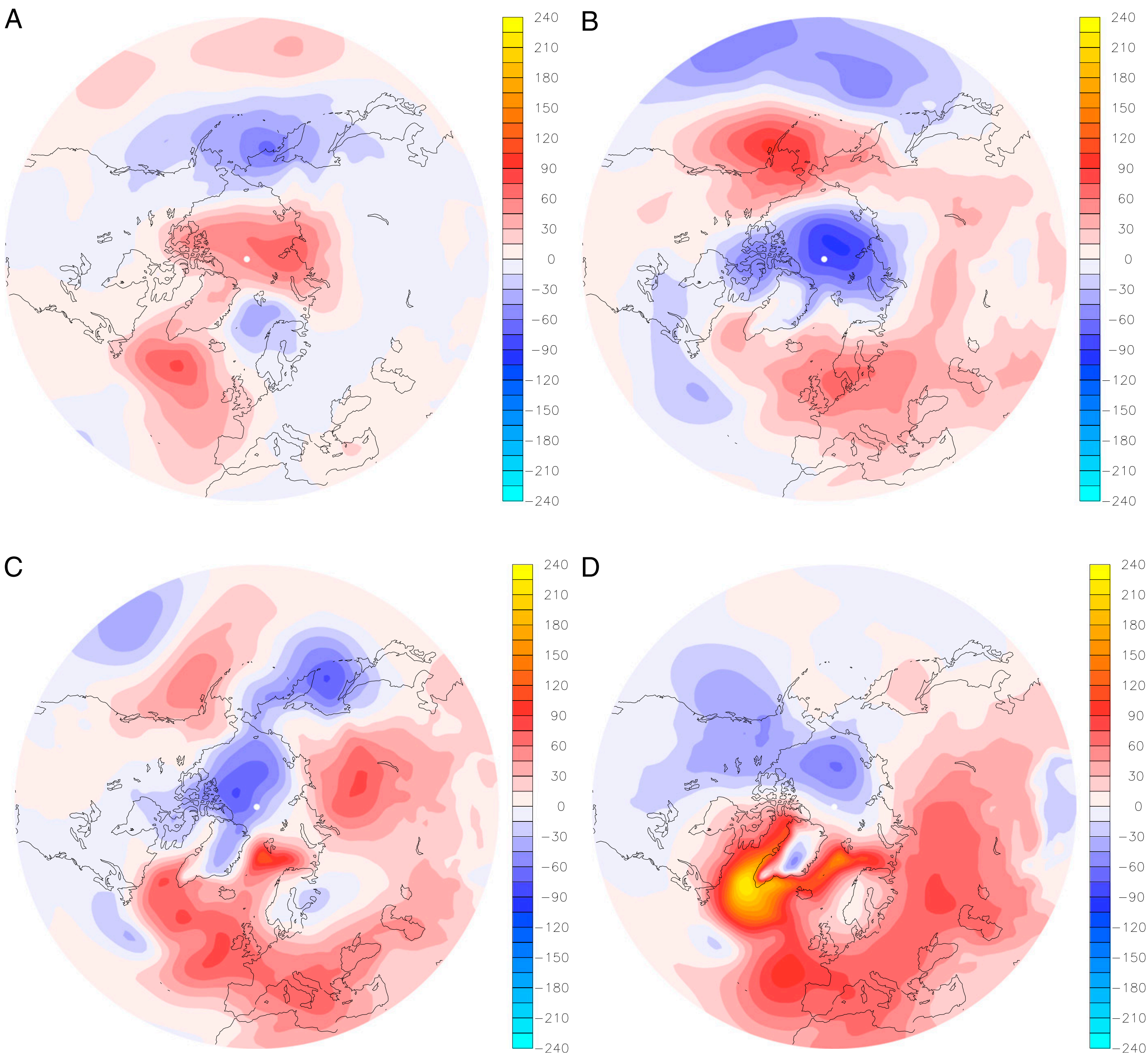

Fig. 3. Stereographic projection of Northern Hemisphere (between 30° and 90°N) SLP anomalies, relative to the climatology of years 200–400. Units are in pascals. (*A*) Twenty-year-averaged SLP anomaly for the years 390–410. (*B*) As in *A*, but for the years 410–430. *A* and *B* show enhanced blocking over the Greenland–Iceland–Norwegian seas, leading to the development of a negative SAT anomaly before the onset of coupled SIC and SLP anomalies near the sea-ice margin. (*C*) Twenty-year-averaged SLP anomaly for the years 430–450 when coupling to SIC anomalies starts, just before the cold event. (*D*) As in *C*, but for the century-averaged SLP anomaly for the years 450–550 during the height of the cold event.

reduced basal melting. From Fig. 2*A* we see that the AMOC did not respond abruptly, but continued to weaken during the cold event, enhancing sea-ice cover in the Labrador Sea. Due to this process a second thermally forced high-pressure anomaly established over the Labrador Sea/northwestern subpolar gyre (Fig. 3*D*), gaining in amplitude relative to the high-pressure anomaly east of Greenland. Once the high-pressure anomaly south of Greenland was fully developed, anomalous southerly winds started to prevail east of Greenland. This terminated the SIC anomaly east of Greenland and the sea-ice thickness anomalies farther north. As a result, the SST and SSS anomalies in the Labrador basin started to diminish as well. The stratification decreased and the AMOC and deep convection recovered. In the last phase of the cold event, the center of the high-pressure anomaly above the Labrador Sea weakened and first moved southeastward; thereafter a high-pressure anomaly established above the North Sea, leaving a low-pressure anomaly above the Arctic (Fig. S4 *A* and *B*) and reestablishing strong westerlies above the Nordic seas.

Uniqueness of the Abrupt Change

After imposing external perturbations sea ice (16) and AMOC (27) can undergo abrupt transitions between multiple equilibria. The changes we described above had a different origin, and the resulting cooling over Europe was similar (28). Here, without an external freshwater perturbation, large amounts of freshwater were transported from the Arctic to the North Atlantic due to a positive feedback between SIC and SLP anomalies east of

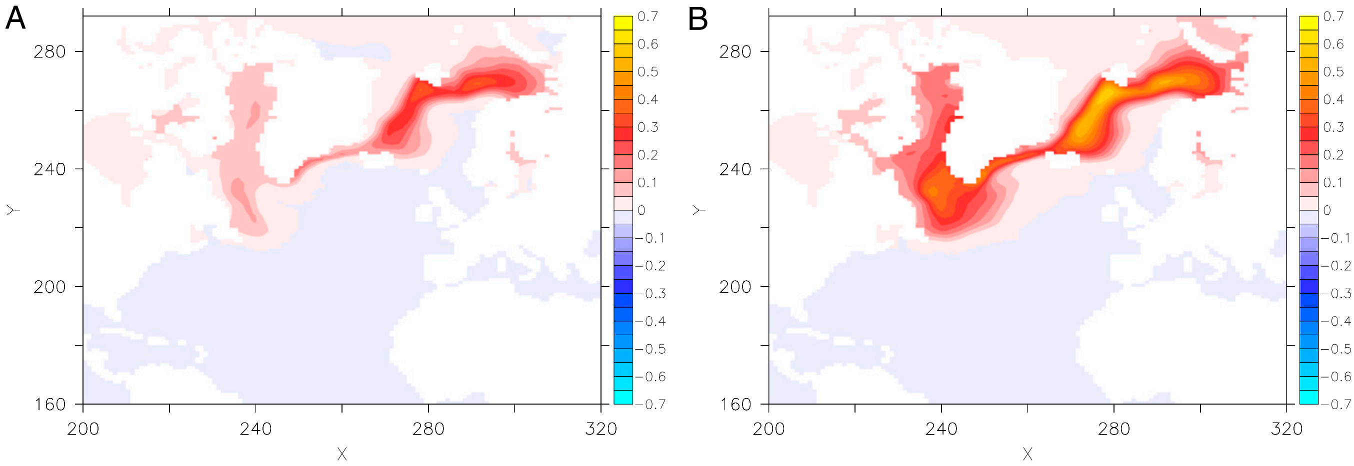

Fig. 4. Sea-ice anomalies associated with the cold event. (*A*) Twenty-year average of annually averaged SIC anomaly for the years 430–450 relative to the climatology for the years 200–400, just before the cold event. (*B*) As in *A*, but for the century-averaged anomaly for the years 450–550, during the height of the cold event. Numbers indicate a fraction of 1.

Greenland. The resulting freshwater anomaly was similar to, but larger than, the Great Salinity Anomaly observed in the late 1960s and 1970s (29). A regime switch between different equilibrium states did not occur. It should be noted, however, that many climate models are biased with respect to the sign of the salt–advection feedback in the ocean, preventing a stable off mode of the AMOC (30). This is also the case for the present simulation. There is no indication that the abrupt change associated with the cold event was associated with the AMOC collapsing to the off mode. Transitions between multiple climate states feature early warning signals, which can be analyzed using statistical techniques (31, 32). Such early warning signals were absent for all fields investigated (SSS, SST, air–sea heat exchange, and AMOC strength), apart from SLP, which showed signs of increased variance before the onset of the cold event (Fig. S5), reflecting the increased feedback through sea ice and winds. From this analysis (Figs. S5 and S6) we infer that the cold event was not due to a switch of the AMOC to another equilibrium state. The most likely explanation for the cold event was the switching on of a quickly growing perturbation due to a suddenly arising instability in the coupled system. Transient amplification occurred when the slowly varying background climate state, in particular its sea-ice distribution, suddenly featured a large correlation with a thermally forced SLP pattern. EC-Earth possesses relatively high resolution in its atmosphere and hence is able to capture atmospheric blocking and its dependence on the background state more realistically (33). The strong atmospheric blocking in response to the SIC anomaly appeared crucial in exciting and maintaining the cold event. This is possibly the reason why a similar event does not appear in other climate models, which

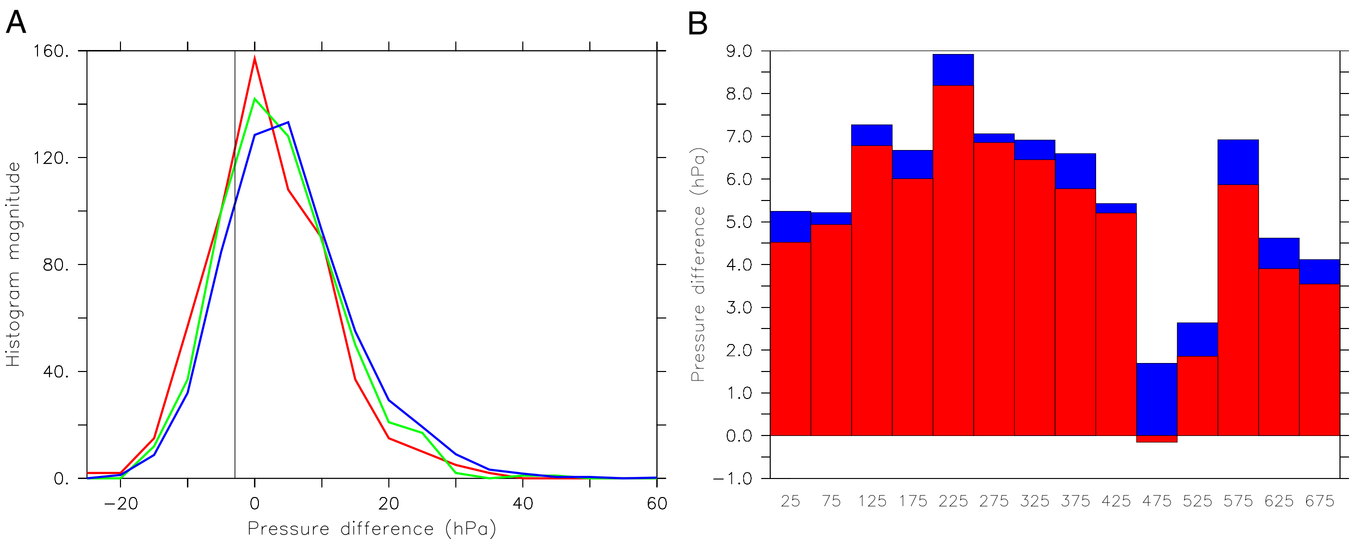

Fig. 5. Blocking characteristics associated with the cold event. To characterize blocking, a pressure index defined by the difference between 10°E and 40°W at 65°N was chosen. Positive values indicate northward flow, negative values indicate southward flow. Statistics were based on monthly mean output as the length of the integration (1,125 y) precluded saving fields at higher frequencies. (*A*) Probability density function of the pressure index in histogram magnitude based on 5-hPa bins. The blue curve is for years 200–400, which is taken as the climatology. The red curve is for the first half of the cold event, years 450–500; the green curve is for the second half of the cold event, years 500–550. The black vertical line separates the blocked regime from the normal regime, defined by the mean minus 1σ from the climatology. (*B*) Bar chart of mean pressure index (red), and means for the normal regime (blue) in hectopascals, for 50-y periods from years 0 to 700 highlighting the negative pressure index anomalies in the years 450–550.

underestimate blocking, or appears there with much weaker amplitude and duration. Fig. S7 shows the SIC before the occurrence of the high spatial correlation between sea ice and SLP. No large biases are evident that single out the model as an outlier with respect to other coupled climate models, although the model does have a cold bias over the Arctic (34).

The multicentury events observed in the Holocene, such as the LIA, differ from the cooling simulated here. This is not surprising because the PI run that we analyzed lacks historical forcing. However, a similar feedback involving interactions between sea ice and the AMOC, amplifying an initial cooling due to explosive volcanism, has been proposed as an explanation for the onset of the LIA (35). Also, a recent analysis of a high-resolution proxy record confirms that the AMOC amplified the LIA event (36). With the present results, we cannot establish whether historical forcing would enhance the likelihood of the abrupt event described above. The main result of this study, however, is that a state-of-the-art climate model can be subject to spontaneous abrupt climate change similar to observed abrupt climate changes, without imposed perturbations. Provided that the correct background state of the coupled ocean–sea-ice system exists (37), strong positive feedbacks can occur temporarily, which amplify specific anomaly patterns. This scenario explaining the abrupt event is very different from stochastic resonance theory (38), because it does not require a system with multiple AMOC equilibria.

Conclusions and Broader Implications

The cold event in EC-Earth crucially depended on the switching on of a strong coupling between SIC and SLP anomalies. This feedback required the ability of sea ice to quickly grow and expand the sea-ice margin. The presence of a strong, southward flowing current (East Greenland Current), and a source of sea ice upstream of the current were crucial. Therefore, it is tempting to speculate that this feedback only works in a climate that is cold enough, which would preclude the occurrence of similar abrupt cold events in present-day and future, warmer climates. The projected decline of the AMOC in warmer climates, however, affects SST and SIC patterns (29). Together with increased freshwater forcing from mass loss from the Greenland Ice Sheet and changing precipitation patterns, it cannot be ruled out that in a future climate strong spatial correlations may occur between SIC and SLP anomalies, leading to spontaneous growth of sea ice. The lesson learned from this study is that the climate system is capable of generating large, abrupt climate excursions without externally imposed perturbations. Also, because such episodic events occur spontaneously, they may have limited predictability.

Furthermore it was shown that an atmosphere feedback associated with century-long enhanced blocking is crucial to enhance and prolong ocean–sea-ice feedbacks. The event as a whole featured different SIC- and SLP-anomaly patterns in its various stages, with feedbacks due to matching of these patterns. As a result, only coupled climate models that are capable of realistically simulating atmospheric blocking in relation to sea-ice variations feature the enhanced sensitivity to internal fluctuations that may temporarily drive the climate system to a state that is far beyond its standard range of natural variability.

ACKNOWLEDGMENTS. We thank Alastair McKinstry of the Irish Centre for High-End Computing for technical support in setting up the EC-Earth model for Met Éireann. The constructive input of two anonymous referees is gratefully acknowledged.

1. Dansgaard W, et al. (1993) Evidence for general instability of past climate from a 250-kyr record. *Nature* 364(6434):218–220.
2. Broecker WS, Bond G, Klas M, Bonani G, Wolfli W (1990) A salt oscillator in the glacial Atlantic? 1. The concept. *Paleoceanogr* 5(4):469–477.
3. Ganopolski A, Rahmstorf S (2001) Rapid changes of glacial climate simulated in a coupled climate model. *Nature* 409(6817):153–158.
4. Schmittner A, Yoshimori M, Weaver AJ (2002) Instability of glacial climate in a model of the ocean- atmosphere-cryosphere system. *Science* 295(5559):1489–1493.
5. Seager R, et al. (2002) Is the Gulf Stream responsible for Europe's mild winters? *Q J R Meteorol Soc* 128(586):2563–2586.
6. Gildor H, Tziperman E (2003) Sea-ice switches and abrupt climate change. *Philos Trans A Math Phys Eng Sci* 361(1810):1935–1944.
7. Denton GH, Alley RB, Comer GC, Broecker WS (2005) The role of seasonality in abrupt climate change. *Quat Sci Rev* 24(10-11):1159–1182.
8. Li C, Battisti DS, Bitz CM (2010) Can North Atlantic sea ice anomalies account for Dansgaard-Oeschger climate signals? *J Clim* 23(20):5457–5475.
9. Ashkenazy Y, Losch M, Gildor H, Mirzayof D, Tziperman E (2013) Multiple sea-ice states and abrupt MOC transitions in a general circulation ocean model. *Clim Dyn* 40(7-8):1803–1817.
10. Laurian A, Drijfhout SS, Hazeleger W, van Dorland R (2009) Global surface cooling: The atmospheric fast feedback response to a collapse of the thermohaline circulation. *Geophys Res Lett* 36(20):L20708.
11. Chiang JCH, Bitz CM (2005) The influence of high latitude ice on the position of the marine intertropical convergence zone. *Clim Dyn* 25(5):477–496.
12. Vellinga M, Wood RA (2002) Global climate impacts of a collapse of the Atlantic thermohaline circulation. *Clim Change* 54(3):251–267.
13. Zhang R, Delworth TL (2005) Simulated tropical response to a substantial weakening of the Atlantic thermohaline circulation. *J Clim* 18(12):1853–1860.
14. Stouffer RJ, et al. (2006) Investigating the causes of the response of the thermohaline circulation to past and future climate changes. *J Clim* 19(8):1365–1387.
15. Clement AC, Peterson LC (2008) Mechanisms of abrupt climate change of the last glacial period. *Rev Geophys* 46(4):1–39.
16. Rose BEJ, Ferreira D, Marshall J (2013) The role of oceans and sea ice in abrupt transitions between multiple climate states. *J Clim* 26(9):2862–2879.
17. Hall A, Stouffer RJ (2001) An abrupt climate event in a coupled ocean-atmosphere simulation without external forcing. *Nature* 409(6817):171–174.
18. Goosse H, Renssen H, Selten FM, Haarsma RJ, Opsteegh JD (2002) Potential causes of abrupt climate events: A numerical study with a three-dimensional climate model. *Geophys Res Lett* 29(18):7-1–7-4.
19. Alley RB, et al. (2003) Abrupt climate change. *Science* 299(5615):2005–2010.
20. Hazeleger W, et al. (2012) EC-Earth V2.2: Description and validation of a new seamless Earth system prediction model. *Clim Dyn* 39(11):2611–2629.
21. Kerr RA (2000) A north Atlantic climate pacemaker for the centuries. *Science* 288(5473): 1984–1985.
22. Van der Schrier G, Barkmeijer J (2005) Bjerknes' hypothesis on the coldness during AD 1790-1820 revisited. *Clim Dyn* 24(4):355–371.
23. Bond G, et al. (1997) A pervasive millennial-scale cycle in North Atlantic Holocene and glacial climates. *Science* 278(5341):1257–1266.
24. Wouters B, Drijfhout SS, Hazeleger W (2012) Interdecadal North-Atlantic meridional overturning circulation variability in EC-Earth. *Clim Dyn* 39(11):2695–2712.
25. Drijfhout SS, van Oldenborgh GJ, Cimatoribus A (2012) Is a decline of AMOC causing the warming hole above the North Atlantic in observed and modeled warming patterns? *J Clim* 25(24):8373–8379.
26. Hoskins BJ, Karoly D (1981) The steady linear response of a spherical atmosphere to thermal and orographic forcing. *J Atmos Sci* 38(6):1179–1196.
27. Huisman SE, den Toom MM, Dijkstra HA, Drijfhout SS (2012) An indicator of the multiple equilibria regime of the Atlantic meridional overturning circulation. *J Phys Oceanogr* 40(3):551–567.
28. Laurian A, Drijfhout SS, Hazeleger W, van den Hurk B (2010) Response of the Western European climate to a collapse of the thermohaline circulation. *Clim Dyn* 34(5): 689–697.
29. Dickson RR, Meinke J, Malmberg SA, Lee AJ (1988) The "Great Salinity Anomaly" in the northern North Atlantic 1968-1982. *Prog Oceanogr* 20(2):103–151.
30. Drijfhout SS, Weber SL, van der Swaluw E (2011) The stability of the MOC as diagnosed from model projections for pre-industrial, present and future climates. *Clim Dyn* 37(7-8):1575–1586.
31. Livina VN, Lenton TM (2007) A modified method for detecting incipient bifurcations in a dynamical system. *Geophys Res Lett* 34(3):L03712.
32. Van der Mheen M, et al. (2013) Interaction network based early warning indicators for the Atlantic MOC collapse. *Geophys Res Lett* 40(11):2714–2719.
33. Scaife AA, Woollings T, Knight J, Martin G, Hinton T (2010) Atmospheric blocking and mean biases in climate models. *J Clim* 23(23):6143–6152.
34. Koenigk T, et al. (2013) Arctic climate change in 21st century CMIP5 simulations with EC-Earth. *Clim Dyn* 40(11–12):2719–2743.
35. Miller GH, et al. (2012) Abrupt onset of the Little Ice Age triggered by volcanism and sustained by sea-ice/ocean feedbacks. *Geophys Res Lett* 39(2):L02708.
36. Wanamaker AD, Jr., et al. (2012) Surface changes in the North Atlantic meridional overturning circulation during the last millennium. *Nat Commun* 3:899, 10.1038/ncomms1901.
37. Tziperman E, Zanna L, Penland C (2008) Nonnormal thermohaline circulation dynamics in a coupled ocean–atmosphere GCM. *J Phys Oceanogr* 38(3):588–604.
38. Alley RB, Anandakrishnan S, Jung P (2001) Stochastic resonance in the North Atlantic. *Paleoceanography* 16(2):190–198.